ACS APPLIED MATERIALS & INTERFACES

Review

www.acsami.org

Multifunctional Fluorescent-Magnetic Polymeric Colloidal Particles: Preparations and Bioanalytical Applications

Chariya Kaewsaneha,[‡,¶] Pramuan Tangboriboonrat,[*,¶] Duangporn Polpanich,[§] and Abdelhamid Elaissari[‡]

[‡]University of Lyon-1 Villeurbanne, CNRS, UMR 5007, LAGEP-CPE, 43 bd 11 Novembre 1918, F-69622 Villeurbanne, France

[¶]Department of Chemistry, Faculty of Science, Mahidol University, Phyathai, Bangkok 10400, Thailand

[§]NANOTEC, National Science and Technology Development Agency (NSTDA), 111 Thailand Science Park, Thanon Phahonyothin, Tambon Khlong Nueng, Amphoe Khlong Luang, Pathum Thani 12120, Thailand

ABSTRACT: Fluorescent-magnetic particles (FMPs) play important roles in modern materials, especially as nanoscale devices in the biomedical field. The interesting features of FMPs are attributed to their dual detection ability, i.e., fluorescent and magnetic modes. Functionalization of FMPs can be performed using several types of polymers, allowing their use in various applications. The synergistic potentials for unique multifunctional, multilevel targeting nanoscale devices as well as combination therapies make them particularly attractive for biomedical applications. However, the synthesis of FMPs is challenging and must be further developed. In this review article, we summarized the most recent representative works on polymer-based FMP systems that have been applied particularly in the bioanalytical field.

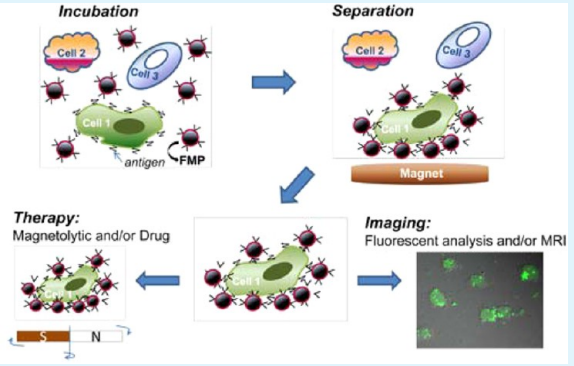

KEYWORDS: *magnetic nanoparticle, fluorophore, hybrid nanoparticle, multifunctional devices, bioanalytical applications*

1. INTRODUCTION

To date, hybrid and/or composite particles bearing remote manipulations of particulate motion in a fast, simple, and precise manner, which is of practical significance in biomedical applications, have been urgently required. For instance, integrating fluorescent and magnetic properties into one entity is of great interest in various systems, such as bioimaging, diagnostics, and therapeutics.[1−6] A number of recent articles have addressed several methods used to fabricate multifunctional particles with the goal of optimizing fluorescent characteristics as well as magnetic or superparamagnetic properties.[7−14] Well-characterized fluorescent-magnetic colloidal particles (FMPs) can serve as fluorescent markers that can be controlled by an external magnetic field as shown in Figure 1.

The process in Figure 1 illustrates the use of FMPs in bioanalytical applications, e.g., diagnosis and therapy of a target cancer cell (Cell 1) in the presence of the other cells (Cells 2 and 3). The colloidal FMPs conjugated with specific targeting groups, i.e., antibodies, can be incubated with the mixture of cancer cells followed by magnetic separation and two detection modes, i.e., magnetic resonance imaging (MRI) and fluorescence analysis. According to the specific antigen labeled on the cell surfaces, the circulating cancer cells can be detected. The high potential FMPs can be used as a therapeutic agent based on magnetolytic therapy, i.e., cancer cells are killed by heat generated from magnetism. Moreover, the FMPs can carry drugs, which will be released with a specific profile to the target cells.

Besides conventional organic dye molecules, e.g., pyrene, rhodamine, and fluorescein isothiocyanate (FITC), fluorescent inorganic nanoparticles, e.g., quantum dots (QDs), can be incorporated inside the FMPs. Each kind of fluorophore has some advantages and limitations.[5,8] Although organic dyes are widely applied in life sciences, several problems, e.g., broad spectral features, short lifetimes, photobleaching, decomposition, and potential cytotoxicity are encountered. Compared with organic dyes, QDs provide high photostability, size-dependent emissions, high quantum yields, and narrow emission bandwidths. However, QDs have not been universally accepted because of their inherent toxic elements (Hg, Cd, Se, Te, In, As, and Pb), chemical instability, and complex conjugation chemistry.

In the past five years, there have been several review articles published on aspects of FMPs ranging from chemical synthesis to surface engineering for biomedical uses.[7,9−14] The obstacle in the combination of fluorophore and magnetic nanoparticles (MNPs) is that fluorescence quenching occurred via an energy transfer process when a fluorophore directly contacts with or is in proximity to the metal oxide surface. For this phenomenon to be avoided, the intermediate layer or spacer is added to separate the magnet and fluorophore, leading to a magnetic core-fluorescent shell morphology.[15−17] Generally, polymer could be used as a matrix, stable isolating layer, or spacer prior

Received: January 23, 2015
Accepted: October 6, 2015
Published: October 6, 2015

DOI: 10.1021/acsami.5b07515
ACS Appl. Mater. Interfaces 2015, 7, 23373−23386

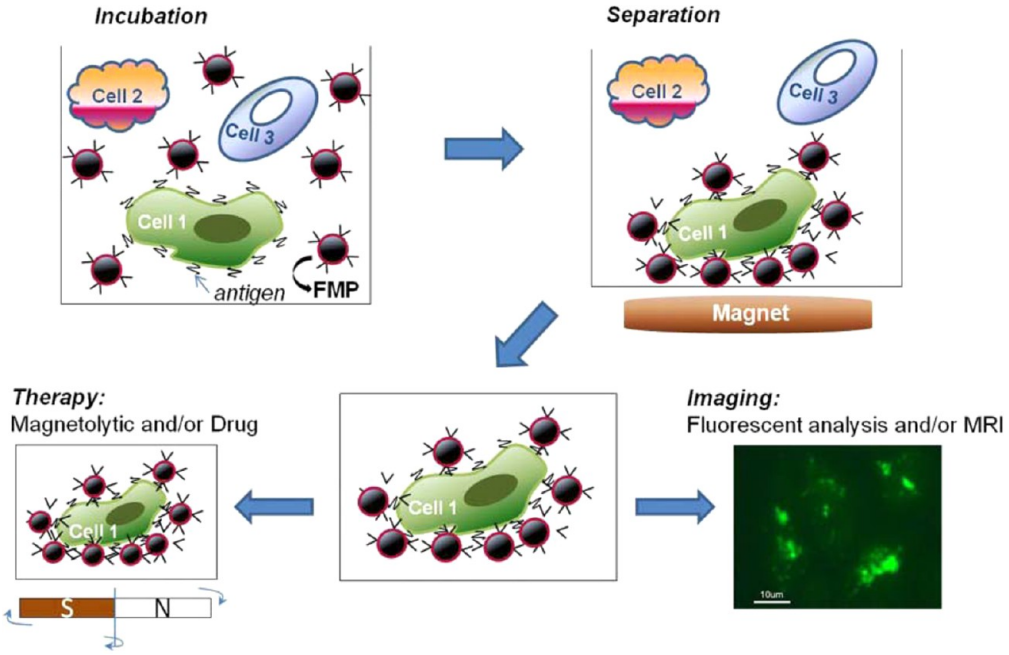

Figure 1. Schematic illustration of multifunctional FMPs used in bioanalytical applications, i.e., cell targeting, separation, imaging, and therapy.

to conjugation with fluorophore molecules. This polymeric layer is preferably employed due to its ease for further functionalization, which makes FMPs useful in advanced bioanalytical applications.[14,18−21] The core−shell structure of FMPs can be both symmetric and asymmetric in shape. Anisotropic-shaped FMPs, i.e., hemispherical, dumbbell-like and/or snowman-like morphologies, have been studied.[22,23] Such architecture reduces the contact of combined individual components such that their magnetic and fluorescent fingerprint properties are not interfered. The hybrid particles showing high potential in nanotechnological applications have rarely been reported.[22,23]

In this review, the focus was on conventional, potential, and recent methods used for the preparation of polymer-based colloidal FMPs with both symmetric as well as asymmetric morphologies published in the time period of 2005−2015. The methods are based on two strategies: encapsulation of fluorophore together with MNPs and polymer-coated magnetic core immobilized with fluorescent entities. The techniques used for synthesis of nano- and micron-sized Janus FMPs were emphasized. The methods to avoid fluorescence quenching effect and releasing of fluorescent dyes from polymer particles were systematically presented. Recent progresses of the polymeric FMPs in bioanalytical applications, i.e., in vitro and in vivo cell labeling and imaging, bioseparation, and in vivo diagnostics and therapy (theranostics), were also described. In addition, the fabricated FMPs for enhanced permeability and retention (EPR) effect and the accelerated clearance phenomenon were included. Abbreviations used in this review are listed in Table 1.

2. PREPARATION OF FMPS

On the basis of the methods used for the preparation of magnetic and/or fluorescent polymeric particles, the encapsulation of MNPs and fluorescent dye inside the same particle prior to surface modification with other active molecules via chemical and/or physical reactions is widely used for the FMP preparation.[24−28] However, this preparative route can reduce or interfere with the functionality of each unit, especially the fluorescence quenching effect. Another strategy to prepare FMPs is a polymer-coated magnetic core immobilized with fluorescent entities.

2.1. Encapsulation of Fluorophores Together with a Magnetic Substance. The encapsulation or incorporation of fluorophores together with MNPs in one particle is the easiest way to produce FMPs. The MNPs and fluorophore dispersed in nano- or micron-sized polymer particles can be fabricated by means of emulsion and/or miniemulsion polymerization, layer-by-layer (LbL) technique, solvent evaporation, and a microfluidic device for large quantity production (Table 2).[12,29−36] Although morphology of FMPs prepared by this concept can improve the properties of MNPs and prevent the MNPs from leaching to the media, the fluorescence quenching due to the close inclusion of magnetic and fluorescent domains is a serious concern.

Poly(lactic-*co*-glycolic acid) (PLGA) entrapping superparamagnetic iron oxide nanoparticles (SPION), manganese-doped zinc sulfide (Mn:ZnS) QDs, and anticancer drug (busulfan) was synthesized via the emulsion-evaporation process. Dichloromethane solution of PLGA, oleic acid (OA)-modified SPION, Mn:ZnS QDs, and busulfan were mixed with a poly(vinyl alcohol) (PVA) aqueous solution. After ultrasonication of oil-in-water (O/W) emulsion and solvent evaporation, FMPs with PVA as a stabilizer were formed. Loading SPION and Mn:ZnS QDs in a PLGA vesicle was clearly demonstrated under a transmission electron microscope (TEM). The fluorescent spectra of the synthesized FMPs revealed the characteristic peak of fluorescence emission at 599 nm originating from the loaded Mn:ZnS QDs, which facilitated further imaging applications.[35]

The LbL technique is another way to encapsulate CdTe QDs and MNPs inside polymer capsules as demonstrated in Figure 2A.[29] The wall of the capsule was first formed by coating alternate layers of oppositely charged polyelectrolytes (PEs), i.e., poly(styrenesulfonate) (PSS) and poly(allylamine hydrochloride) (PAH), on a melamine formaldehyde (MF) core.

DOI: 10.1021/acsami.5b07515
ACS Appl. Mater. Interfaces 2015, 7, 23373−23386

Table 1. Summary of Abbreviations

abbreviation	name
AA	acrylic acid
CET	Cetuximab
CMC	carboxymethyl chitosan
CS	chitosan
DTX	docetaxel
EGF	epidermal growth factor
EPR	enhanced permeability and retention
FITC	fluorescein isothiocyanate
FMNHs	fluorescent magnetic nanohybrids
FMPs	fluorescent-magnetic colloidal particles
GMA	glycidyl methacrylate
HEMA	2-hydroxyethyl methacrylate
HFMA	2,2,3,4,4,4-hexafluorobutyl methacrylate
LbL	layer-by-layer
MNPs	magnetic nanoparticles
MPNPs	magnetic polymeric nanoparticles
MRI	magnetic resonance imaging
MW	molecular weight
NIPAM or NIPAAM	*N*-isopropylacrylamide
OA	oleic acid
OPE	oligo(*p*-phenyleneethynylene)
PAH	poly(allylamine hydrochloride)
PCL	poly(ε-caprolactone)
PE	polyelectrolyte
PEG	poly(ethylene glycol)
Phen	1,10-phenanthroline
PLGA	poly(lactic-*co*-glycolic acid)
PMAA	poly(methacrylic acid)
PMI	*N*-(2,6-diisopropylphenyl)-perylene-3,4-dicarbonacidimide
PS	polystyrene
PSS	poly(styrenesulfonate)
PSSS	poly(sodium-4-styrenesulfonate)
PVA	poly(vinyl alcohol)
Py-PEG	pyrene polyethylene glycol
QDs	quantum dots
RAFT	reversible addition−fragmentation chain transfer
SPION	superparamagnetic iron oxide nanoparticle
St	styrene
TCL	thermally cross-linked polymer
VBK	9-(4-vinylbenzyl-9H-carbazole)

Then, the core particle was etched before infiltration of CdTe and Fe_3O_4 nanoparticles into the preformed PE capsules.

Using this technique, MNPs were entrapped in the capsule and existed on the capsule wall because of the electrostatic interaction between acidic moieties of the stabilizers and amino groups of PAH molecules. No leakage of MNPs into the surrounding solution was found, and the images of nanoparticle-loaded capsules observed using a confocal laser scanning microscope TCS Leica in transmission (left column) and luminescence (right column, excitation wavelength 476 nm) modes are shown in Figure 2B. This aforementioned method is simple and allows for the fabrication of different types of multifunctional capsules. However, its drawback was the use of QDs whose fluorescence does not last for more than 2 weeks in physiological buffer solutions.[29]

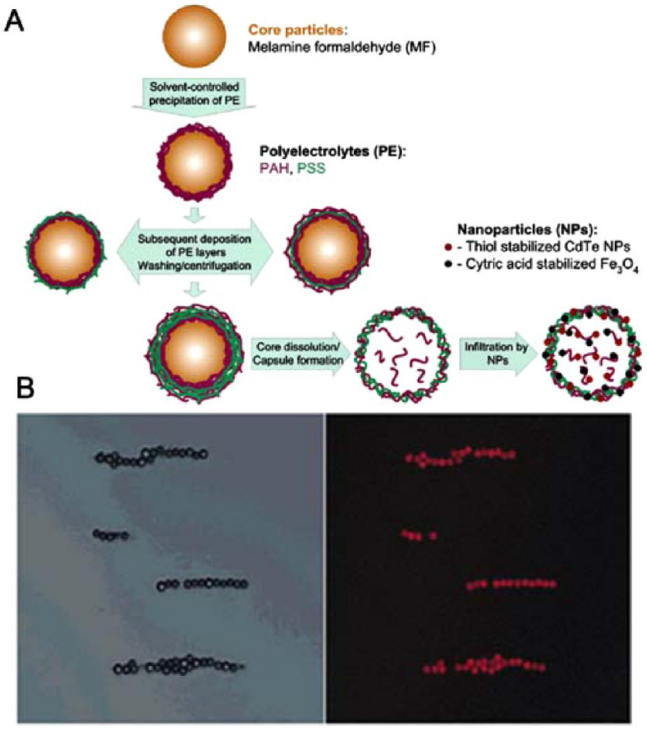

Figure 2. (A) Fabrication of microcapsule and encapsulation of CdTe QDs and Fe_3O_4 nanoparticles via the LbL technique. (B) CdTe and Fe_3O_4-loaded microcapsules were aligned in a magnetic field. The images were obtained with a confocal laser scanning microscope TCS Leica operating in transmission (left column) and in luminescence (right column, excitation wavelength 476 nm) modes. Reproduced with permission from ref 29. Copyright 2004 American Chemical Society.

In another promising method, MNPs and fluorophore were embedded together with in situ polymerization.[12] MNPs and *N*-(2,6-diisopropylphenyl)-perylene-3,4-dicarbonacidimide (PMI) were encapsulated in polystyrene-*co*-acrylic acid (PS-*co*-AA) matrix by the three-step miniemulsion process. The

Table 2. FMPs Prepared using Encapsulation of Fluorophore together with a Magnetic Substance

polymer	fluorophore	magnetic species	method	ref
PLGA	Mn:ZnS QDs	Fe_3O_4	emulsion-evaporation method	35
PSS and PAH	CdTe QDs	Fe_3O_4	layer-by-layer technique	29
PS-*co*-AA	PMI	Fe_3O_4	three-step miniemulsion process	12
PCL-*b*-PMAA	pyrene	$MnFe_2O_4$	nanoemulsion method	30
PEG-diacrylate	rhodamine B	Fe_3O_4	microfluidic device-based method	31
poly(styrene-*b*-allyl alcohol) (PS_{16}-*b*-PAA_{10})	pyrene	hydrophobic MNPs	solvent evaporation-based method	33
PS	1-pyrene carboxaldehyde	Janus magnetic emulsion	swelling diffusion method	36
PS	fluorescein dimethacrylate	OA-coated MNPs having Triton X-405 at the surface	in situ seed emulsion polymerization	36

DOI: 10.1021/acsami.5b07515
ACS Appl. Mater. Interfaces 2015, 7, 23373−23386

obtained particles showed homogeneity with magnetic content up to 40 wt % and demonstrated fluorescent properties of PMI in cell labeling applications. The pores of these particles were large enough to accommodate both MNPs and PMI fluorescent dye. Similarly, water-soluble nanohybrid FMPs consisting of $MnFe_2O_4$ magnetic nanocrystals encapsulated in pyrene-labeled poly(ε-caprolactone)-*b*-poly(methacrylic acid) (PCL-*b*-PMAA) as a surfactant were synthesized by the nanoemulsion method.[30] The pyrene-labeled PCL-*b*-PMAA was first synthesized as a phase transfer agent. By using this amphiphilic block copolymer as a surfactant, the MNPs and pyrene-labeled groups were forced to gather inside the polymer particles. FMPs (112 nm) surrounding active functional groups (−COOH and − COO^-) showed a response to both a magnetic field and emitting fluorescence signal. To potentially use the prepared FMPs as a cancer-imaging probe, antibody (Cetuximab) was further conjugated on the surface of the particles.

For a large quantity of FMPs with micron-sized regime to be produced, the microfluidic device-based method was then introduced.[31,32] For example, Yuet et al. prepared a hydrogel microparticle possessing fluorescent and magnetic properties on opposite sides, which was called the Janus particle.[31] The term "Janus" was inspired from the Roman God Janus, with two heads placed back to back, looking to the future and the past. This term was extended to encompass colloidal particles that have different properties at opposite sides. This asymmetrical morphology offers unique features and provides advanced multifunctionality, e.g., composition, hydrophobicity, and hydrophilicity, combined and modular functionalities, which enable important applications unavailable to their symmetrical counterparts.[22,23] The principle of this technique relies on a Y-shaped channel to form a two-phase monomer stream with a planar sheath-flow geometry. Monodisperse droplets are easily formed at the junction of the microchannels by controlling the flow rates of the dispersed and continuous phases as shown in Figure 3A. Two streams of mineral oil sheared off monodisperse droplets of two UV curable polymeric streams: (i) nonmagnetic poly(ethylene glycol)-diacrylate solution (PEG-DA) containing rhodamine B fluorescent dye and (ii) PEG-DA solution containing MNPs. Downstream of the flow-focusing region and a step-change in the channel height from 20 to 70 μm allowed the droplets to relax into spheres, which were subsequently polymerized upon UV irradiation.

Figure 3B displays that the Janus spherical particles having separately located rhodamine B and MNPs inside particle (48 μm) were generated at a throughput of ca.10^5 particles per hour. This controllable field-driven assembly of the particles can be potentially used as building blocks to construct targeted, superstructures for tissue engineering. This method also showed the ability to generate multifunctional Janus particles with great design flexibilities: (a) direct encapsulation and precise spatial distribution of biological substances and (b) selective surface functionalization in a particle. Although these monodisperse particles are promptly used in tissue engineering, their ability to self-assemble with tunable anisotropic configurations makes them an intriguing material for several exciting areas of research such as photonic crystals, novel microelectronic architecture, and sensing.

Although the microfluidic methods based on a phase separation strategy can be scaled-up to produce a large quantity of Janus FMPs in a continuous fashion, the sizes of the resulting particles are relatively large ranging from one to hundreds of

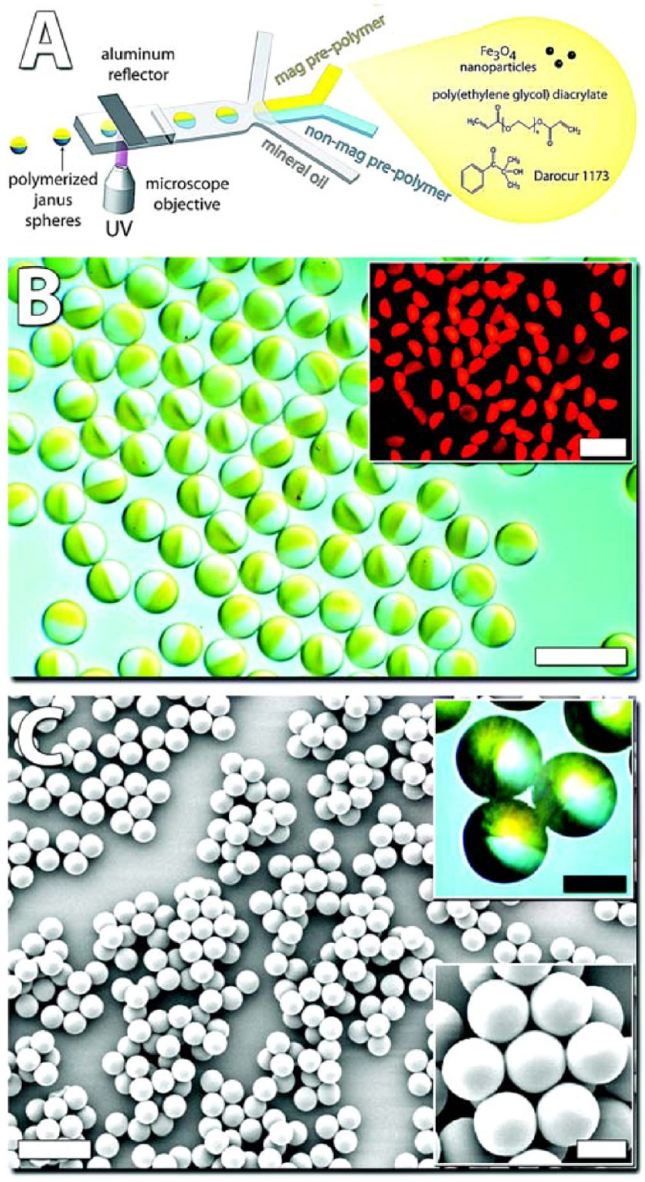

Figure 3. (A) Schematic illustration of Janus particle synthesis in a flow-focusing microfluidic device. (B) Digital camera and corresponding fluorescence (insert) images of magnetic Janus particles generated from coflowing streams of polymer, one containing MNPs and the other containing rhodamine B. The scale bars are 100 μm. (C) Scanning electron microscope and DIC (upper right insert) images of dried Janus particles. Reproduced with permission from ref 31. Copyright 2010 American Chemical Society.

micrometers due to the relatively large fluidic channels. Thus, another improved method to produce nanohybrid FMPs with Janus morphology, i.e., the solvent evaporation method, was introduced as schematically illustrated in Figure 4A.[33]

MNPs and pyrene-labeled poly(styrene-*b*-allyl alcohol) were dissolved in chloroform and then emulsified in aqueous medium in the presence of PVA as stabilizer. After slow evaporation of solvent, phase separation between MNPs and fluorescent-labeled polymer matrix occurred, leading to the formation of spherical FMPs containing MNPs located on one side and fluorescent molecules on the other side. The orientation of hybrid nanoparticles was controlled by an

DOI: 10.1021/acsami.5b07515
ACS Appl. Mater. Interfaces 2015, 7, 23373−23386

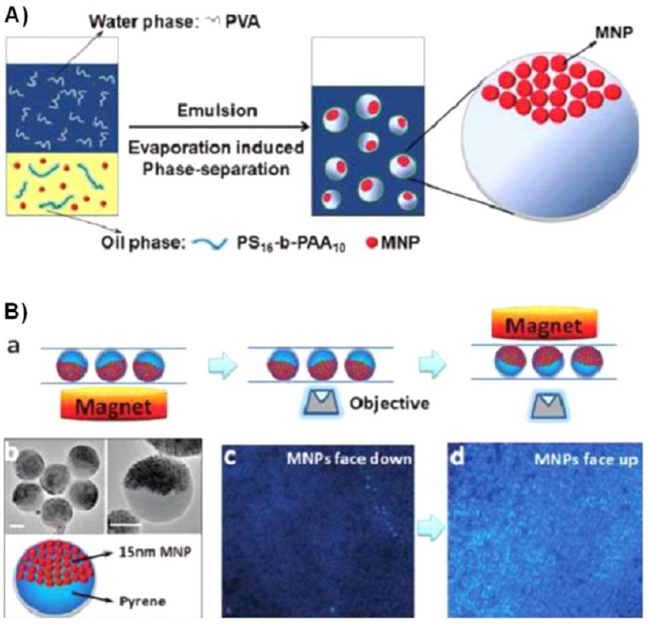

Figure 4. (A) Schematic illustration of the key steps involved in the synthesis of multifunctional nanocomposites with spatially separated functionalities using the solvent evaporation method. (B) Orientation-dependent fluorescence of nanohybrid FMPs. (a) Schematic of nanoparticles with magnetic fields. The magnetic segment blocked both excitation and fluorescence when it was facing down but had no effect on fluorescence when facing up (not in the light path). (b) TEM images of the nanoparticles with the two phases of similar volume. The scale bars are 100 nm. (c and d) Fluorescence imaging of nanoparticles of opposite orientations. Reproduced with permission from ref 33. Copyright 2010 American Chemical Society.

external magnetic field, and the fluorescent signal was observed as shown in Figure 4B.

Additionally, nanosized Janus FMPs can be fabricated using the swelling-diffusion and the in situ seed emulsion polymerization method. In the swelling-diffusion process, Janus magnetic emulsion was prepared via emulsion polymerization in the presence of St monomer and oil-soluble 2,2′-azobis(2-isobutyronitrile) (AIBN) initiator. It was subsequently used as seed, which allowed the diffusion of 1-pyrenecarboxaldehyde (PyCHO) fluorescent dye dissolved in organic solvent after incubating overnight. After solvent evaporation, Janus FMPs were obtained. Both the type and quantity of organic solvents were important parameters to produce the particles with high fluorescence intensity as well as to maintain Janus morphology. Well-defined Janus morphology and narrow size distribution of Janus particles were obtained only when THF was used. In the case of the in situ seed emulsion polymerization method, styrene (St), fluorescein dimethacrylate (FDMA), and AIBN were used as main monomer, fluorescent comonomer, and initiator, respectively, whereas OA-coated MNPs possessing Triton X-405 at the surface were applied as a seed emulsion. Because of the incompatibility of magnetic seed emulsion and PS, phase separation between polymer and magnetic emulsion was enhanced. Confocal microscopy confirmed the strong fluorescence intensities of the hybrid particles prepared via both techniques. However, the advantage of the in situ seed emulsion polymerization method involved the uniform distribution of dye along the polymer backbone via chemical bonding, which inhibited the leakage of fluorescent dye out of the particle.[36]

2.2. Polymer-Coated Magnetic Core Immobilized with Fluorescent Entities. Coating the polymer shell on a single or aggregated MNP core before introducing fluorophore offers a promising solution to prevent the quenching effect. The interaction between polymer coating and fluorophore can be either physical or chemical. The potential methods used for synthesis of core−shell FMPs are displayed in Table 3.

The multilayered coating around the MNP core via the LbL technique allows tuning of polymer-coating thickness and the deposition of charged particles or molecules.[34,37] For example, Hong et al. prepared luminescent nanocomposites comprised of Fe_3O_4 MNP core (8.5 nm) and CdTe QDs/polyelectrolyte (PE) multilayers via the LbL assembly approach as shown in

Table 3. FMPs Prepared using Polymer-Coated Magnetic Core Immobilized with Fluorescent Entities

polymer	fluorophore	magnetic species	method	type of interaction between fluorophore and polymer or surface of FMPs	ref
PSS and PAH	CdTe QDs	Fe_3O_4	LbL	physical	34
PSSS and PAH	rhodamine B	Fe_3O_4	LbL	physical	37
CS	FITC	γ-Fe_2O_3	coating of FITC-CS onto γ-Fe_2O_3 surface	chemical	40
CMCS	FITC	γ-Fe_2O_3	coating of FITC-CMCS onto silica-coated γ-Fe_2O_3 surface	chemical	21
commercial polymer having −SH and −COOH	CdSe/ZnS	γ-Fe_2O_3	organic/water two-phase mixture	chemical	15
poly(St-*co*-GMA)	europium complex ($Eu(AA)_3Phen$)	Fe_3O_4	two-step, seed emulsifier-free emulsion polymerization technique	chemical	43
Poly(St-NIPAM)	$Eu(AA)_3Phen$	Fe_3O_4	two-step, seed emulsifier-free emulsion polymerization technique	chemical	44
P(HEMA)@P(NIPAAM-*co*-AA)	FITC	Fe_3O_4	combination of sol−gel, distillation precipitation polymerization (DPP), and RAFT polymerization process	chemical	45
PEG	1-pyrene butyric acid	Aggregated $MnFe_2O_4$	self-assembly	chemical	41
poly(HFMA-*co*-VBK) -*g*-PEG	VBK	Fe_3O_4 cluster	self-assembly	chemical	46
poly(styrene/divinylbenzene/acrylic acid) and CS	FITC	Fe_3O_4	miniemulsion polymerization	chemical	42

DOI: 10.1021/acsami.5b07515
ACS Appl. Mater. Interfaces 2015, 7, 23373−23386

Figure 5A.[34] The number of PE multilayers separating the nanoparticle layers and the number of QDs/PE deposition

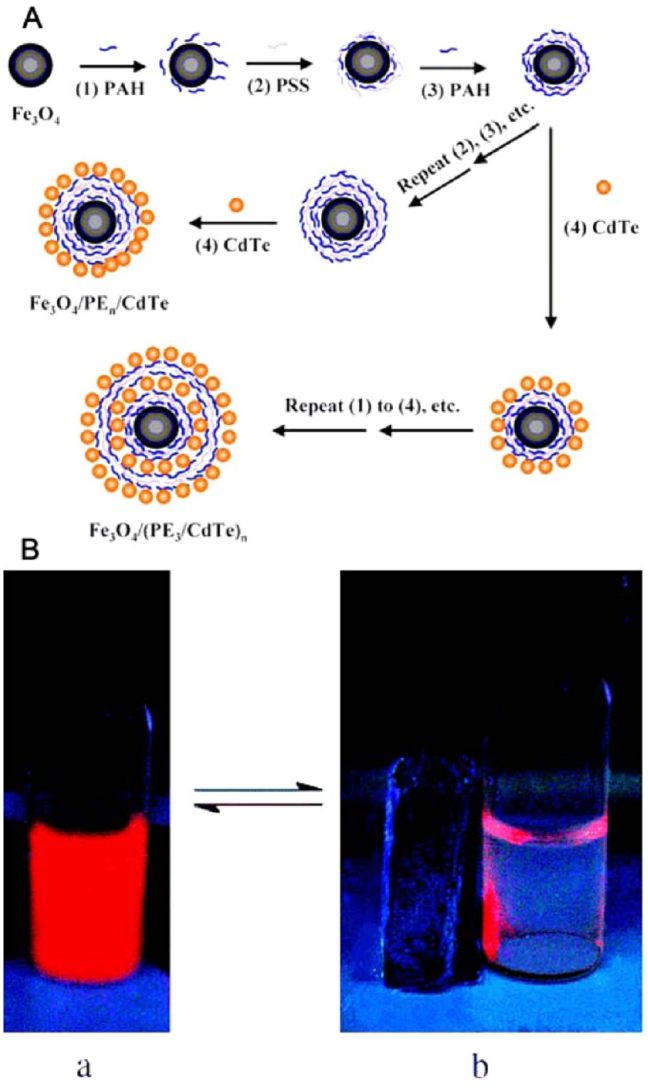

Figure 5. (A) Schematic illustration of the LbL process forming magnetic luminescent nanocomposites. (B) Photographs of magnetic luminescent nanocomposites under UV irradiation (a) without and (b) with an external magnetic field. Reproduced with permission from ref 34. Copyright 2004 American Chemical Society.

cycles were varied to produce two types of magnetic luminescent nanocomposites, $Fe_3O_4/PE_n/CdTe$ and $Fe_3O_4/(PE_3/CdTe)_n$. By using this technique, the selection of a certain number of inserted PE interlayers and CdTe QD loading on the nanocomposites could optimize the photoluminescence properties of the nanocomposites. Hence, the nanocomposites were easily separated and collected in an external magnetic field with a highly emitted luminescent signal under irradiation as shown in Figure 5B. With removal of the magnetic field followed by vigorous stirring, the aggregations were rapidly redispersed. It should be mentioned that the magnetic properties of the nanocomposites also made them possible for site-specific transport.

Similarly, Gallagher et al. prepared bimodal FMP nanostructures using the LbL technique.[37] Magnetite nanoparticles (Fe_3O_4) were initially produced by reacting a mixture of Fe^{2+} and Fe^{3+} and poly(sodium-4-styrenesulfonate) (PSSS) aqueous solution with ammonia. The magnetite-PSSS nanomaterials were alternately coated with positively charged PAH and negatively charged PSSS polyelectrolyte multilayers (10 layers in total). Then, a positively charged rhodamine B layer was deposited on the last negatively charged PSSS layer. However, the stability of the obtained particles was limited (only 3 days) due to the weak ionic interaction between dye and the particle surface, which precluded their use in biomedical applications.

The strategies for such hybrid nanoparticles require elaborate chemical processes, including coupling the fluorophore to a nanoparticle by covalent linkage.[21,38−42] Polymers containing functional groups, such as carboxylic acid and amino groups, can be effectively conjugated to the functional fluorescent dyes. The biopolymer chitosan (CS) covalently bound to FITC (FITC-CS) was synthesized and subsequently coated on the γ-Fe_2O_3 MNP surface (FITC-CS@MNP) for cellular imaging.[40] The reaction was based on the isothiocyanate group of FITC and primary amino group of CS. However, the fluorescence intensity of the FITC-CS@MNP was lower than that of the FITC-CS due to the quenching effect. Because low molecular weight (MW) CS was employed, the chance that FITC molecules were in proximity to the MNP surface was high, and energy transfer was then initiated. By coating the γ-Fe_2O_3 MNP surface with silica and subsequently with carboxymethyl CS before labeling by FITC, the increased distance prevented the quenching effect between the MNP surface and FITC molecules.[21]

Wang et al. described the formation of luminescent and magnetic nanocomposites consisting of superparamagnetic core particles (γ-Fe_2O_3) and a layer of luminescent CdSe/ZnS QDs on their surface via an organic/water two-phase mixture.[15] The commercial polymer-coated MNPs were functionalized with dimercaptosuccinimide acid (DMSA) containing free thiol (−SH) and carboxyl (−COOH) residues to enable covalent coupling of the QDs and ligand to separate and subsequently detect breast cancer cells. The particles, with an average diameter of 20 nm and ∼15% size variation, showed relatively smooth morphology and were fully miscible with water. They also exhibited high emission quantum yield and were easily separated from solution when applying a permanent magnet.

Furthermore, Zhu et al. successfully produced FMPs via the two-step, seed emulsifier-free emulsion polymerization technique.[43] Fe_3O_4/poly(styrene-*co*-glycidyl methacrylate) (St-*co*-GMA) nanoparticles were first synthesized as seeds, and then fluorescent europium complex containing three double bonds, $Eu(AA)_3Phen$, was copolymerized with the remaining St and GMA to form the outer fluorescent polymer shell. Besides good cytocompatibility, the obtained FMPs exhibited excellent superparamagnetic and fluorescent properties. Using a similar technique, bilayered OA and sodium undecylenate (NaUA)-modified Fe_3O_4 MNPs incorporated in thermoresponsive and fluorescent $Eu(AA)_3Phen$ poly(St-*N*-isopropylacrylamide) (St-NIPAM) shell were synthesized.[44] NaUA presented on the surface of MNPs not only enhanced the particle stability via electrostatic interactions stemming from its negatively charged carboxylate moieties, but also rendered the modified MNPs accessible for monomers, which brought about effective encapsulation. In addition, it was found that magnetic fluid and $Eu(AA)_3Phen$ contents played a crucial role in controlling the size and morphology of the final composite particles.

Recently, Torkpur-Biglarianzadeh et al. introduced temperature and pH-responsive properties to FMPs and tested their use in a drug delivery system in which $Fe_3O_4@SiO_2@P(2-$

DOI: 10.1021/acsami.5b07515
ACS Appl. Mater. Interfaces 2015, 7, 23373−23386

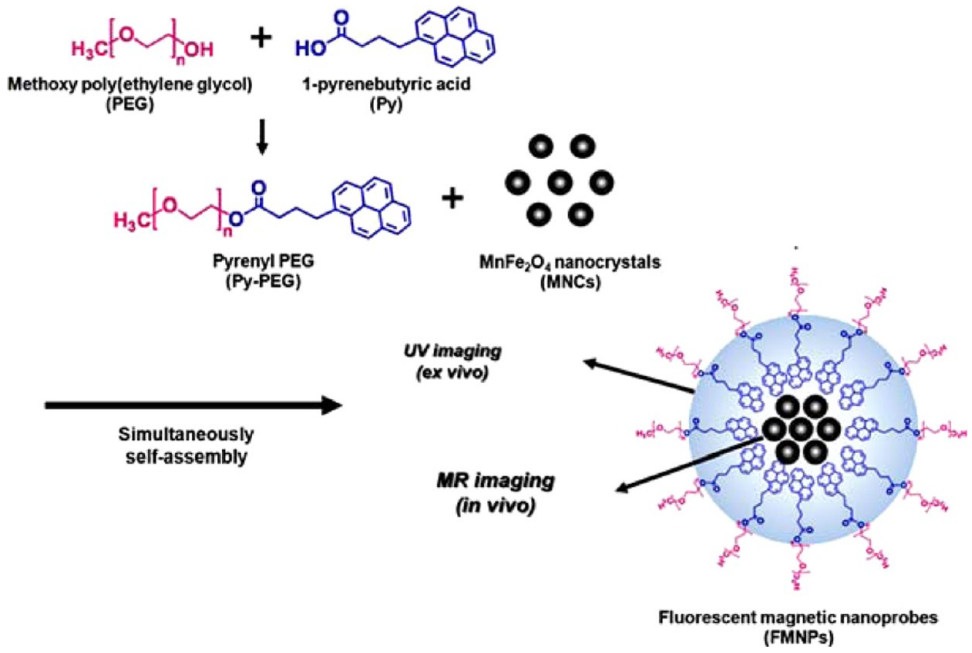

Figure 6. Schematic illustration of simultaneous self-assembled fluorescent magnetic nanoparticles as multimodal biomedical imaging probes. Reproduced with permission from ref 41. Copyright 2010 Elsevier.

hydroxyethyl methacrylate)@P(*N*-isopropylacrylamide-*co*-acrylic acid) (Fe_3O_4@SiO_2@P(HEMA)@P(NIPAAM-*co*-AA)) nanoparticles were synthesized via the combination of sol−gel, distillation precipitation polymerization (DPP), and reversible addition−fragmentation chain transfer (RAFT) polymerization processes.[45] Fe_3O_4@SiO_2@P(HEMA) was first synthesized through a sol−gel process of tetraethyl orthosilicate and FITC-conjugated 3-aminopropyltriethoxysilane followed by DPP of HEMA and *N*,*N*′-methylenebis(acrylamide). After conjugation with folic acid (FA) (cancer-cell specific targeting) and RAFT agent, polymerization of NIPAAM and AA took place to fabricate Fe_3O_4@SiO_2@P(HEMA)@P(NIPAAM-*co*-AA) nanoparticles. The nanoparticles showed well-defined core−shell morphology with dazzling green fluorescence. The presence of multilayers of polymer did not influence their superparamagnetic properties. A clear suspension at 15 °C and a turbid suspension at 45 °C confirmed the thermoresponsiveness of the nanocomposites. Their solubility in aqueous medium can be altered by changing pH, which associated with the presence of P(HEMA) and PAA. In addition, high loading of anticancer drug and controllable drug, which was attributed to the presence of P(NIPAAM-*co*-AA) and a cross-linked P(HEMA) shell, was observed.

For MNP-based bioanalytical applications, a large amount of MNP core is required. In this case, the MNP core should be aggregated or encapsulated inside a single matrix before introducing the fluorophore shell. Figure 6 displays one example of FMP nanoprobes synthesized using amphiphilic pyrenyl polyethylene glycol (Py-PEG) as the fluorophore and aggregated superparamagnetic $MnFe_2O_4$ nanocrystals as the core.[41] Py-PEG synthesized by conjugation of hydrophilic PEG with hydrophobic and fluorescent 1-pyrenebutyric acid through an esterification process was capable of self-assembly, and it still maintained a high fluorescence intensity in the aqueous phase. Py-PEG, a fluorescent surfactant, efficiently encapsulated MNPs to form nanocomposites possessing fluorescence and magnetic properties as well as high solubility in water. The obtained particles clearly showed not only biocompatible and nontoxic characteristics but also excellent magnetic resonance (MR) sensitivity and high illumination intensity with strong signal strength under short exposure time of UV light from the extensive imaging studies.

Additionally, Chu et al. synthesized poly(2,2,3,4,4,4-hexafluorobutyl methacrylate-*co*-9-(4-vinylbenzyl)-9*H*-carbazole)-*g*-polyethylene glycol (poly(HFMA-*co*-VBK)-*g*-PEG) copolymer using free radical polymerization to encapsulate OA-modified Fe_3O_4 clusters.[46] On the basis of self-assembly of the amphiphilic copolymer, hydrophobic HFMA had a high tendency to penetrate into the OA shell of the magnetic cluster and face out the hydrophilic VBK and PEG segments, which served as the fluorescent unit and stabilizer, respectively, to the aqueous phase upon encapsulation. The increase in fluorine content in poly(HFMA-*co*-VBK)-*g*-PEG copolymer brought about the high loading efficiency of MNPs until reaching a certain fluorine concentration. The prepared FMPs with an average size of 146 nm possessed good superparamagnetic properties and showed vivid blue fluorescence from the carbazole unit. However, the emission spectra of Fe_3O_4-encapsulated poly(HFMA-*co*-VBK)-*g*-PEG revealed that fluorescence intensity of the particles decreased when the particle concentration was higher than 0.9 mM due to self-quenching and magnetism of Fe_3O_4.

It is worth noting that the thin coating layer might be insufficient to protect the fluorescence quenching effect and to prevent the oxidation of the metal particle and would be less stable at high temperature. Therefore, encapsulation of MNPs in polymer matrix, i.e., magnetic polymeric nanoparticles (MPNPs) prior to immobilization of fluorescent species is important.[42] Besides avoiding direct contact between MNPs and the media or the fluorophore, the surface of MPNPs can be further modified for specific uses in bioanalytical applications. For example, the carboxylated MPNPs containing MNPs homogeneously dispersed in poly(styrene/divinylbenzene/acrylic acid) matrix were prepared via miniemulsion polymer-

DOI: 10.1021/acsami.5b07515
ACS Appl. Mater. Interfaces 2015, 7, 23373−23386

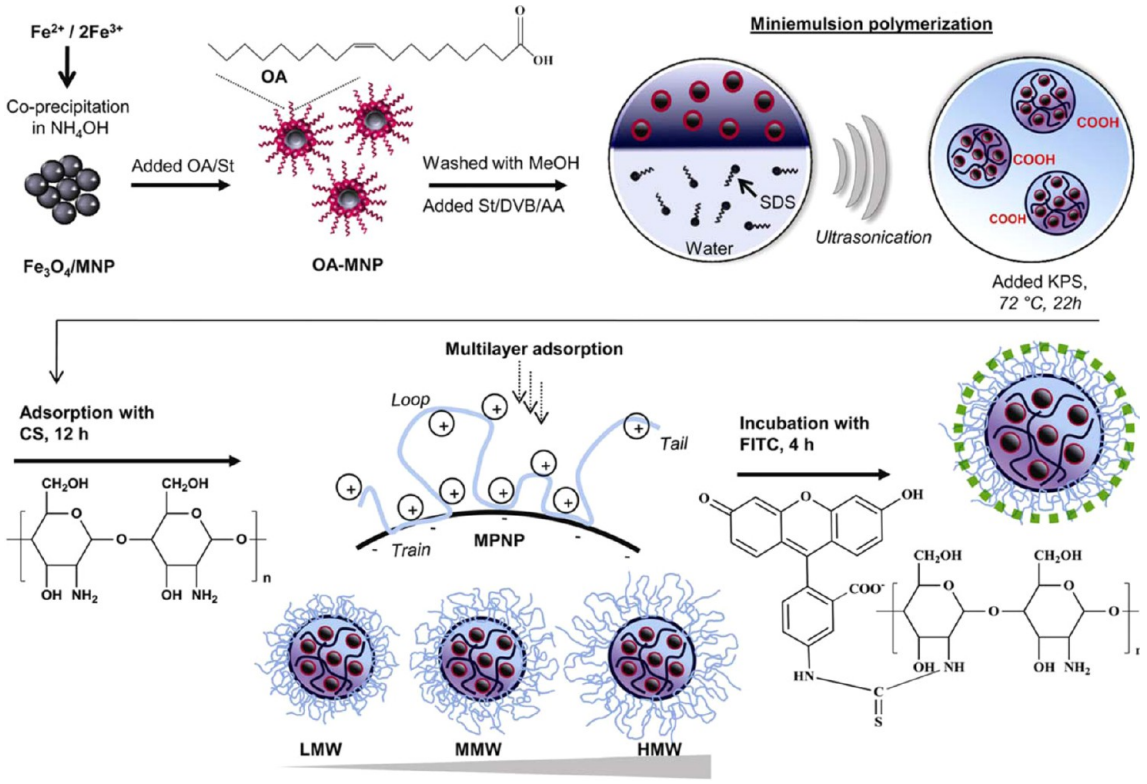

Figure 7. Schematic representing the preparation of FMPs using the miniemulsion polymerization process followed by CS coating and conjugation with FITC. Reproduced with permission from ref 42. Copyright 2012 Elsevier.

ization. Potassium persulfate and divinylbenzene were used as water-soluble initiator and cross-linking agent, respectively, to prepare high content of MNPs (41%) uniformly dispersed in polymer matrix. The biopolymer, CS, was then coated on the carboxylated MPNPs via electrostatic interaction between negatively charged MPNPs and positively charged CS. Because of the high deacetylation degree of CS, the residual active functional groups of CS ($-NH_2$) were chemically reacted with the isothiocyanate group of FITC. By using a proper MW of CS spacer, the FMPs having high magnetic content and fluorescence intensity without the quenching effect were obtained as presented in Figure 7.

3. BIOANALYTICAL APPLICATIONS

The hybrid colloidal FMPs bearing magnetic and fluorescent properties have proven to be a potential candidate in the biomedical arena, e.g., in vitro and in vivo cell labeling and imaging, bioseparation, and in vivo diagnostics and cancer therapy.[47−52] Because of the dual detection modes, i.e., fluorescence and magnetism, the use of nanoscale colloidal FMPs as a multimodal probe would provide the high impact in nanotechnology. The parallel detection provides a clearer picture and correct diagnosis compared with the previous approaches, which may require the process of fixed tissue samples.[5] Moreover, polymer-based FMPs, having a size in the range of 200 nm or below, have shown promising progress in bioimaging and cancer therapy due to the presence of the inherent leakiness of the tumor vascular barrier and dysfunctional lymphatic system, called the EPR effect, in which the nanoparticles are preferentially accumulated at specific tumor sites through passive targeting.[53,54]

3.1. Cell Labeling and Imaging. Several works reported the use of hybrid colloidal FMPs as a dual contrast reagent. The idea is to use these particles as probes to obtain directional information about cell-particle interactions in nonspecific and specific targeting fashions. For example, the FMPs containing fluorescein and rhodamine fluorescent dyes were used for cellular imaging.[10] After cellular uptake, the particles were confined inside endosomes, which are submicron vesicles of the endocytotic pathway. Moreover, the magnetic manipulation of these particles was clearly observed under confocal microscopy by the formation of spectacular fluorescent chains aligned in the direction of the applied magnetic field.

Another work considered biocompatible nanohybrid FMPs as bioimaging probes. The FMPs composed of an MNP core coated with FITC-modified CS were used for cellular imaging.[40] Cancer cells (SMMC-772) were labeled with the biocompatible nanoparticles, i.e., FITC-CS@MNP FMPs, which served as both MR contrast agent for MRI and the optical probe for intravital fluorescence microscopy. With a clinical 1.5T MR imager, the MR images of samples in Eppendorf tubes were evaluated. Under T_2* weighted image mode (T_2* WI), cells exposed to 15.44 μg of the FMPs for 2 h could be easily detected as shown in Figure 8A. These labeled cells could be visualized in a clinical 1.5T MR imager with detectable cell numbers of $\sim 10^4$ in vitro. To clarify the location of FMPs in the cells, the authors performed fluorescence and electron microscopy. It was observed that the particles were located inside the cells as well as on the cell surface as presented in Figure 8B and C. Hence, binding a fluorescent dye to MNPs enabled their direct imaging and localization in living cells. Similarly, γ-Fe_2O_3 MNPs coated with aminopropyl-containing silica or partially carboxymethyl CS (γ-Fe_2O_3−SiO_2-AP-CMCS) were used for both MR and fluorescence molecular imaging as a powerful tool to study the interaction of the nanoparticles with biological systems. Besides demonstrat-

DOI: 10.1021/acsami.5b07515
ACS Appl. Mater. Interfaces 2015, 7, 23373−23386

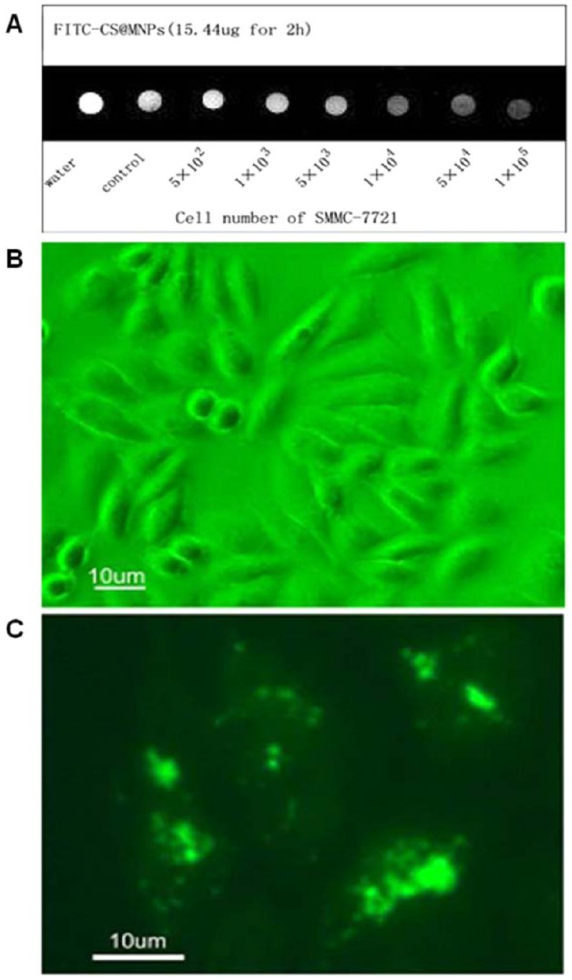

Figure 8. (A) T_2* imaging of different numbers of cells when labeled with FITC-CS@MNP FMPs in vitro. Cell concentrations ranging from 5×10^2 to 1×10^5 cells after treatment with 15.44 μg of FMPs for 2 h were scanned. Unlabeled cells of identical numbers and distilled water were also scanned as a control group. (B and C) Fluorescence images of SMMC-7721 cells when incubated with (B) control and (C) FMPs for 8 h. Reproduced with permission from ref 40. Copyright 2009 Springer.

ing the in vitro use of particles, the labeled particles can be used for in vivo visualization after being injected into a rat brain.[21] The cell implant was clearly visible on the MR image as a hypointense spot with excellent contrast against the surrounding tissue as observed in Figure 9a and b. Histology in Figure 9c confirmed the deposition of iron oxides in the cell implant that corresponded to the results from Prussian Blue staining. The cell implant was also visible under a fluorescence microscope as illustrated in Figure 9d. Such labeling offered the possibility of tracking cells by MRI and fluorescent microscopy in cell cultures or even in living organisms.

Furthermore, dual in vivo imaging of cancer cells labeled with Cy5.5-conjugated, thermally cross-linked polymer (poly(3-(trimethoxysilyl)propyl methacrylate-*r*-PEG methyl ether methacrylate-*r*-*N*-acryloxysuccinimide)/SPION (Cy5.5 TCL-SPION) was demonstrated in Figure 10.[52] When the particles were intravenously injected into the rat through its tail vain, the tumor was unambiguously detected in T_2-weighted MRI as a 68% signal drop compared to preinjection as well as in optical fluorescence images within 4 h, indicating a large accumulation

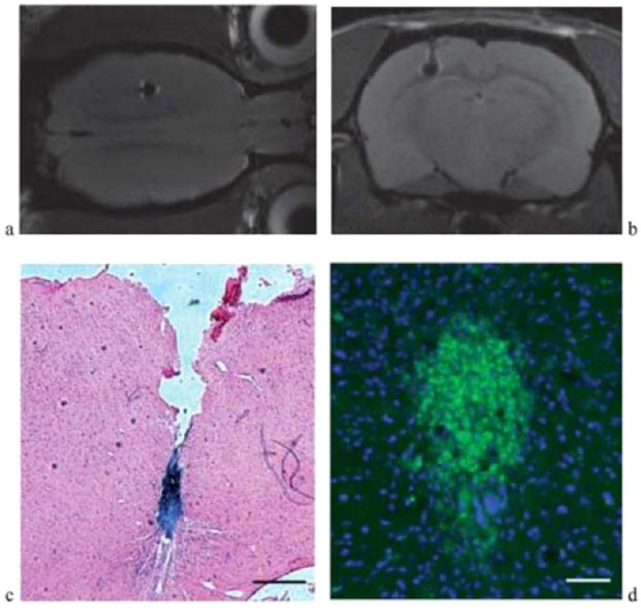

Figure 9. (a) Coronal and (b) axial MRI from rat mesenchymal stem cells labeled with FTIC-labeled γ-Fe_2O_3−SiO_2-AP-CMCS nanoparticles. (c) Cell implant stained for iron using Prussian Blue. Scale bar 0.5 mm. (d) Cell implant visualized in a fluorescence microscope (green); DAPI (blue) stained cell nuclei. The scale bars are 50 μm. Reproduced with permission from ref 21. Copyright 2011 The Royal Society of Chemistry.

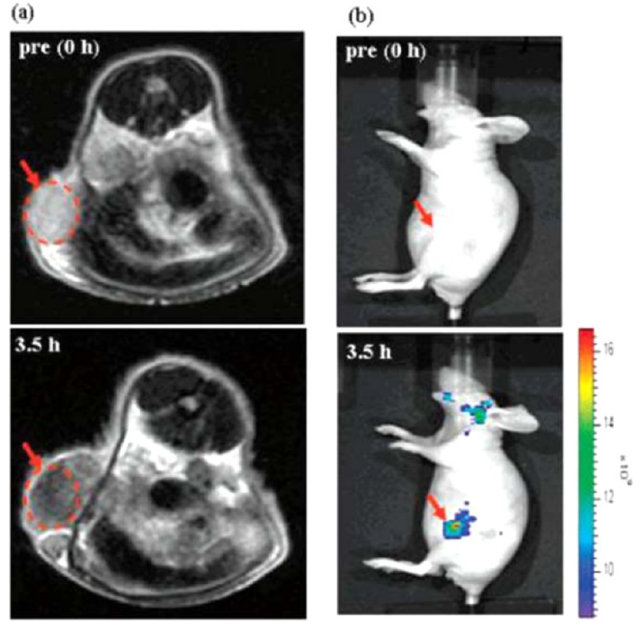

Figure 10. (a) T_2-weighted fast spin−echo image taken at 0 and 3.5 h postinjection of 14.7 mg of Cy5.5 TCL-SPION at the level of tumor (320 mm^3) on the flank above the upper left thigh of a nude mouse and (b) optical fluorescence images of the same mouse taken at 0 and 3.5 h. The red arrows indicate the position of the allograft tumor. Reproduced with permission from ref 52. Copyright 2007 American Chemical Society.

of the Cy5.5 TCL-SPION residing in the tumor. In addition, ex vivo fluorescence images of the harvested tumor and other major organs further confirmed the highest accumulation of the Cy5.5 TCL-SPION within the tumor, which was supposed to

DOI: 10.1021/acsami.5b07515
ACS Appl. Mater. Interfaces 2015, 7, 23373−23386

be due to the EPR effect. The cross-linked structure and antibiofouling property of the polymer layer of Cy5.5 TCL-SPION yielded high stability in physiological medium and high resistance to uptake by cells of the reticuloendothelial system organs, such as liver and spleen. Consequently, their circulation time was long enough to accumulate in the desired tumor tissue without using any specific targeting ligands.

Another effective in vivo imaging probe for tumor detection was reported by Lee et al. They synthesized iron oxide nanoparticle (ION)-loaded OA-conjugated CS conjugated with Cy5.5 near-infrared (NIR) dye having a diameter of 86.1 nm.[55] After intravenous injection through the tail vein of tumor-bearing mice, the prepared FMPs displayed high signal intensity in both near-infrared fluorescence and MR imaging via the EPR effect. In vivo near-infrared fluorescence images of the tumor-bearing mice confirmed the accumulation of nanoparticles at the tumor site. The fluorescence intensity of the tumor tissue continuously increased up to 5 h postinjection and was obviously observed up to 1 day. The fluorescence signal of the tumor tissue was significantly higher than that of normal muscle. In addition, ex vivo near-infrared fluorescence imaging demonstrated no accumulation of nanoparticles in other organs, including the heart, spleen, bone, and muscle.

For the targeting specificity to be improved, the surface of FMPs should be modified or conjugated with specific molecules, e.g., antibody, to interact with specific antigen on the target cells. For example, cetuximab-conjugated fluorescent magnetic nanohybrids (CET-FMNHs) were synthesized for the detection of human epithelial cancer.[30] The carboxylated FMNs composed of aggregated $MnFe_2O_4$ core coated with pyrene-PCL-poly(methyl methacrylate) amphiphilic block copolymer were conjugated with CET antibody, epidermal growth factor (EGF) receptors, and a targeting moiety specific to human epithelial cancer cells as presented in Figure 11A. For investigation of the cancer cell-targeted efficacy, the CET-FMNHs were incubated with A431 cells (high expression of EGF receptor cancer marker) or MCF7 (low expression of the cancer marker) using human IgG-conjugated FMNHs (IgG-FMNHs) as a control. Fluorescence intensity of the treated MCF7 cells showed minimal shift, which was similar to nontreated cells, whereas A431 cells treated with CET-FMNHs demonstrated a higher relative FI compared with IgG-FMNH-treated cells as shown in Figure 11B (a and b, respectively). Furthermore, the A431 cells incubated with CET-FMNHs emitted a fluorescence signal and showed better MR contrast than the treated MCF7 cells and both cells incubated with control IgG-FMNHs.

Liu et al. synthesized magnetic/upconversion fluorescent $NaGdF_4$:Yb,Er nanocrystals (5.1 and 18.5 nm) coated with PEG.[56] The upconversion fluorescent counterpart is favorable for in vivo imaging as near-infrared excitation, which can better penetrate into tissue than visible light and hence gives rise to drastically reduce background noise.[56,57] PEGylated $NaGdF_4$:Yb,Er nanoparticles showed excellent colloidal stability in Milli-Q water as well as phosphate-buffered saline. Afterwards, to increase tumor accumulation, monoclonal anti-EGF receptor antibody was covalently attached to the nanoparticles via the click reaction. In vivo imaging was conducted both intraperitoneally and in subcutaneously xenografted tumors using the BALB/c nude mouse model. Strongly shortened T_1 values of the tumor regions indicated that enhancement of MR contrast was greatly increased by the antibody-functionalized PEGylated $NaGdF_4$:Yb,Er nanoparticles in both tumor models,

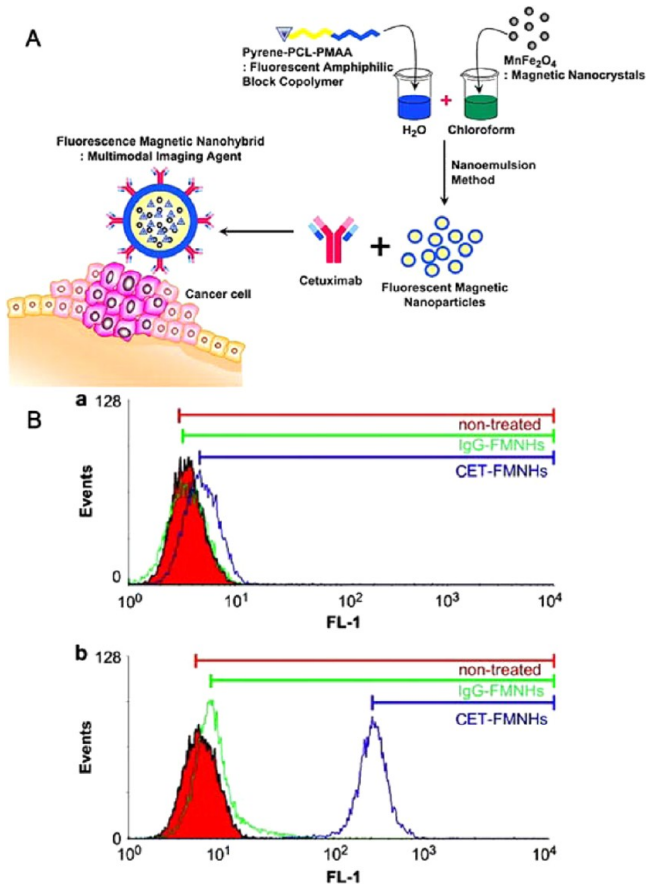

Figure 11. (A) Schematic illustration as multimodal imaging agents for cancer detection. (B) Fluorescence-activated cell sorting analysis of (a) A431 and (b) MCF7 cells; red, nontreated cells; green, IgG-FMNH-treated cells; and blue, CET-FMNHs. Reproduced with permission from ref 30. Copyright 2008 Elsevier.

which was probably caused by the EPR effect. Results from true-color upconversion fluorescence images revealed the strong emission intensity of the functionalized FMPs 8 h postinjection. Interestingly, owing to the excellent properties of the synthesized nanoparticles, subcutaneous tumors smaller than 2 mm were clearly identified in vivo. Pharmacokinetic studies revealed that the elimination pathway of these nanoparticles is particle size dependent. Because the small size of $NaGdF_4$:Yb,Er nanocrystals (5.1 nm) took the renal elimination pathway, the biological half-time was estimated to be 1.4 days, whereas the biological half-time of the larger sized nanoparticles (18.5 nm) was ~8.2 days according to fecal excretion.

MNPs coated with PEG-modified phospholipid micelle structure that was conjugated with fluorescent Texas red dye and Tat-peptide were used for the imaging of primary human dermal fibroblast cells and Madin-Darby bovine kidney derived cells. The particles showed high efficiency to conjugate various moieties for specific intracellular and tissue imaging.[58]

More recently, MNPs encapsulated in fluorescent oligo(*p*-phenyleneethynylene)-PEG-FA (MNPs@OPE-PEG-FA) shell were synthesized for targeting MR and two-photon optical imaging in vitro and in vivo.[59] The OPE having a large two-photo absorption (2PA) cross-section offers deeper tissue penetration and less photobleaching and photodamage, whereas PEG can avoid fast clearance of particles from the immune

DOI: 10.1021/acsami.5b07515
ACS Appl. Mater. Interfaces 2015, 7, 23373−23386

system and FA molecules act as a cancer-targeting ligand. Using a mouse tumor model, compared with the T_2-weighted images of HeLa tumors before MNPs@OPE-PEG-FA injection, an obvious decrease in signal intensity could be detected 4 h after injection. In addition, the MRI T_2 signals of the tumor area were more significantly enhanced. High accumulation of particles induced by FA suggested their effective targeting capability.

3.2. Bioseparation. FMPs can not only be used as multimodal probes but also in bioseparations under magnetic field modulation.[6] The FMPs, prepared by incorporation of MNPs into PS particles before being coated with CdTe QDs, were conjugated with EGF (MNPs/CdTe-EGF) for labeling and separating the specific human breast cancer MDA-MB-435S cells. The MNPs/CdTe-EGF bioconjugates binding to the overexpressed EGF receptor cancer cells could be applied simultaneously for cell labeling and separation.

3.3. Theranostic Applications. For theranostic (diagnostic and therapeutic) applications of FMPs, the fluorescent unit was used for optical diagnostics, and the magnetic part was used for therapy. Incorporation of therapeutic agents, i.e., small drug molecules or SiRNA, into the FMPs is also a key point of theranostic materials. The utilization of polymer-based FMPs for cancer therapy has been extensively studied. It is believed that the highly dispersible and biocompatible FMPs are able to enhance drug efficacy compared with free drugs. The encapsulation of drug and on-site delivery prolong circulation half-life, and sustain or trigger drug release.[60]

The Janus FMPs were studied as for imaging and magnetolytic therapy for cancer cells as shown in Figure 12a.[33] On the basis of magnetic modulation (the orientation strategy for cell imaging application), cell-particle attachment was achieved through nonspecific adsorption facilitated by magnetic manipulation as clearly observed in Figure 12b under a fluorescence microscope. For investigation of the therapeutic effect of the particles through magnetic field-modulated damage of cell membranes, cells were placed in a spinning magnetic field (50 rpm), which generated a mechanical force on the cell membrane. After 15 min of exposure to the spinning magnetic field, the majority of the tumor cells were killed and identified by Trypan blue staining as shown in Figure 12f. Figure 12c indicated that the number of living cells after magnetolytic therapy compared with that of the control was reduced by 77%, whereas those missing either nanocomposites or magnetic field in Figure 12d and e showed >99.5% cell survival.

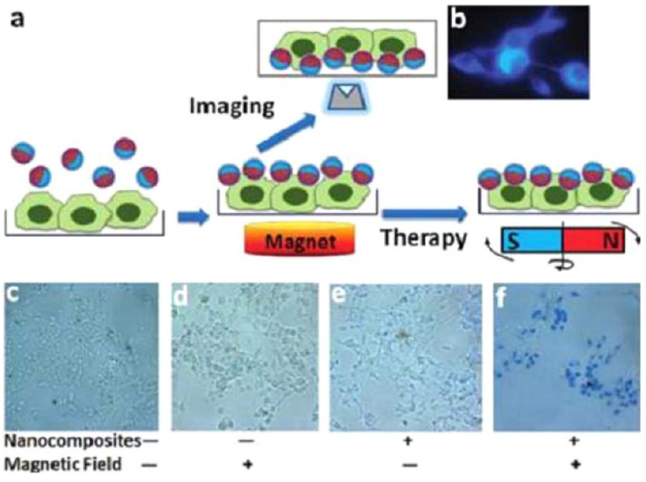

Figure 12. (a) Schematic representation of the experimental conditions and magnetolytic therapy. Nanohybrid FMPs were brought down to the cell surface by magnetic attraction with nonspecific interaction. (b) Fluorescence imaging of cells coated with nanocomposites. (c, f) Magnetolytic therapy on tumor cells (dead cells appear blue due to Trypan blue staining) (f) resulting in dead cells. The number of living cells in (f) compared with that in (c) was reduced by 77%, whereas those in (d) and (e) showed greater than 99.5% cell survival. Reproduced with permission from ref 33. Copyright 2010 American Chemical Society.

Although the hybrid particles with Janus morphology offer high potential for use in bioanalytical fields, a few applications of Janus FMP-based polymer systems have been reported. The performance as biomarkers of Janus FMPs, such as Au/Fe_3O_4 and/or Ag/Fe_3O_4, was explored by selective binding with live tagged cells enabling detection, magnetic recovery, and therapy.[61,62]

The innovative FMPs not only present fluorescence diagnostic and magnetic separation but also carry drugs for specific therapy. PLGA particles encapsulated SPION, Mn:ZnS QDs, and busulfan, an anticancer drug synthesized via emulsion-evaporation process, were applied for drug delivery and imaging. After incubating with J774A murine macrophage cells, the particles exhibited high cellular uptake efficiency. Fluorescence intensity was detected within 2 h and a reached maximum intensity at 24 h of incubation. The high value of transverse relaxivity for PLGA-SPION-Mn:ZnS vesicles, 523 s^{-1} mM^{-1} Fe, indicated their high efficiency for MR T_2* imaging. The vesicles demonstrated high entrapment efficiency for the lipophilic drug busulfan and sustained drug release. These results revealed the capacity of the synthesized particles for delivery of chemotherapeutic agents into the cells as well as their usefulness as an optical imaging agent.[35]

Selective surface functionalization plays a critical role in imaging probes for providing novel simultaneous targeting capabilities, complex drug release profiles, and smart imaging competence. Dumbbell-like gold/magnetite (Au/Fe_3O_4) nanoparticles served as a multifunctional platform for target-specific platin delivery into Her2-positive breast cancer cells.[61] The presence of two different surfaces of the nanoparticle within one nanostructure facilitates the controlled functionalization of each particle. The platin complex was anchored on the optical Au side and the Her2-specific monoclonal antibody Herceptin chosen as a targeting agent was linked to Fe_3O_4. The release of the therapeutic platin under low pH conditions allowed the nanoparticles to conjugate and be more toxic to the targeted tumor cells than free cisplatin. These carriers were achieved as target-specific delivery through strong antibody−antigen interactions and receptor-mediated endocytosis.

There have been reports on the use of polymer-based theranostic multifunctional nanoparticles in nanotechnology, for example, targeted imaging, separation, and photothermal destruction of rare tumor cells from the whole blood sample.[63] The magnetic-gold core−shell star-shaped nanoparticles were coated with thiolated polyethylene glycol (HS-PEG) and then functionalized with aptamer to avoid nonspecific interactions with blood cells. In this case, magnetic core was used for cell isolation and enrichment, and the star shape of gold plasmonic shells was used as both a photothermal agent and a nanoplatform. Because of surface roughness, star-shaped magnetic-plasmonic particles certainly enhanced protein corona attachment, cellular uptake, and magnetic separation capability. The Cy3 fluorescence probe-modified S6 aptamer was attached

DOI: 10.1021/acsami.5b07515
ACS Appl. Mater. Interfaces 2015, 7, 23373−23386

to the magnetic-plasmonic theranostic nanoparticle for specific SK-BR-3 breast cancer cell recognition. Whole blood sample spiked SK-BR-3 cells showed that Cy3-attached S6 aptamer-conjugated theranostic nanoparticles could be used for fluorescence imaging and magnetic separation even in 0.001% mixtures. A targeted photothermal experiment of the particles using 1064 nm near-IR light at 2−3 W/cm^3 for 10 min exhibited selective irreparable cellular damage to most of the SK-BR-3 cancer cells. The theranostic-driven assay would have enormous potential for applications as a contrast agent and therapeutic actuators for cancer.

In recent studies, theranostic nanoparticles composed of the anticancer drug docetaxel (DTX) and magnetic manganese oxide (MnO) nanoparticles encapsulated with fluorescent dye-labeled amphiphilic polymer for dual modal imaging and chemotherapy were developed.[64] The hydrophobic side chain of the polymer was likely to interact with hydrophobic DTX drug, enabling high loading efficiency, whereas its hydrophilic backbone facilitated the dispersion of the nanoparticles in aqueous phase. Results from human breast cancer cell (MDA-MB-231) uptake indicated the accumulation of the particles in cell cytoplasm, and the uptake occurred through energy-dependent endocytosis pathways as observed for other polymer-based nanoparticle systems. At 48 h, ∼50% of DTX was released from the particles. The sustained release of DTX can provide a prolonged therapeutic effect, avoiding the need for frequent administration of nanoparticle formulation. From in vivo biodistribution (mouse model), a strong whole-body fluorescence signal remained for up to 7 days, indicating accumulation and prolonged retention of the particles. Considerable clearance of particles via the renal route occurred within the first 24 h.

4. CONCLUSIONS AND REMARKS

Polymeric colloidal particles composed of fluorescence and magnetic properties were exploited in materials science and bioanalytical applications. The multifunctional FMPs can be controlled by an external magnetic field to be guided to a targeted area and reside there until the diagnostic or treatment is completed prior to removal of an external stimuli. All processes can be monitored by MRI and fluorescence microscopy allowing for full control over the processes. Moreover, if the particles are significantly small but can still integrate magnetic and fluorescent properties without interfering with the detection, they would open up the unique possibility of controlled target-directed applications. This is of particular importance in medicine, as one major disadvantage of any nanoparticles in therapy is the problem of getting the particle to the site of interest.

FMPs have been prepared by various synthetic approaches mainly based on the encapsulation of fluorescence together with MNPs in polymer matrix and fabrication of a polymer-coated magnetic core immobilized with fluorescent entities strategies. The first is the easiest way to produce the FMPs and is an effective method ensuring full incorporation between MNPs and fluorophores, which reduces their being washed off in media. However, it risks a fluorescence quenching effect due to the closing of fluorescence and magnetic domains. The coating of MNPs with a protective shell or a polymer spacer before the attachment of fluorophore for the latter method has been employed as this approach could provide an appropriate distance between the fluorophore and the surface of MNPs. Besides using polymer as matrix and spacer, the functionalization of polymers is the important step to improve the efficiency of FMPs. The use of biocompatible and/or biodegradable polymers makes polymer-based FMPs more attractive as benign as well as smart nanomaterials in the nanotechnology field.

The serious fluorescence quenching effect is still the main problem for combining the two properties within one particle, which is a significant challenge to overcome and to obtain such high potential particles for use in more specific fields, particularly in biomedicine. However, despite all the recent progress, the FMP area is still in an infancy stage, and significant efforts are needed for further development of these materials and their utilizations.

AUTHOR INFORMATION

Corresponding Author

*Tel.: +66-2-2015135. Fax: +66-2-3457151. E-mail: pramuan.tan@mahidol.ac.th.

Notes

The authors declare no competing financial interest.

ACKNOWLEDGMENTS

The authors thank and appreciate the research grant (RTA5480007) from the Thailand Research Fund (TRF)/Commission on Higher Education to P.T. and the scholarship from TRF, Mahidol University, and the French Government through the Royal Golden Jubilee Ph.D. Program (Grant No. PHD/0174/2552) to the PhD student C.K.

REFERENCES

(1) Yi, D. K.; Selvan, S. T.; Lee, S. S.; Papaefthymiou, G. C.; Kundaliya, D.; Ying, J. Y. Silica-coated Nanocomposites of Magnetic Nanoparticles and Quantum Dots. *J. Am. Chem. Soc.* **2005**, *127*, 4990−4991.

(2) Weissleder, R.; Kelly, K.; Sun, E. Y.; Shtatland, T.; Josephson, L. Cell-specific Targeting of Nanoparticles by Multivalent Attachment of Small Molecules. *Nat. Biotechnol.* **2005**, *23*, 1418−1423.

(3) Zebli, B.; Susha, A. S.; Sukhorukov, G. B.; Rogach, A. L.; Parak, W. J. Magnetic Targeting and Cellular Uptake of Polymer Microcapsules Simultaneously Functionalized with Magnetic and Luminescent Nanocrystals. *Langmuir* **2005**, *21*, 4262−4265.

(4) Mailänder, V.; Landfester, K. Interaction of Nanoparticles with Cells. *Biomacromolecules* **2009**, *10*, 2379−2400.

(5) Corr, S. A.; Rakovich, Y. P.; Gun'ko, Y. K. Multifunctional Magnetic-fluorescent Nanocomposites for Biomedical Applications. *Nanoscale Res. Lett.* **2008**, *3*, 87−104.

(6) Chu, M.; Song, X.; Cheng, D.; Liu, S.; Zhu, J. Preparation of Quantum Dot-coated Magnetic Polystyrene Nanospheres for Cancer Cell Labelling and Separation. *Nanotechnology* **2006**, *17*, 3268−3273.

(7) Bigall, N. C.; Parak, W. J.; Dorfs, D. Fluorescent, Magnetic and Plasmonic-hybrid Multifunctional Colloidal Nano Objects. *Nano Today* **2012**, *7*, 282−296.

(8) Quarta, A.; Di Corato, R.; Manna, L.; Ragusa, A.; Pellegrino, T. Fluorescent-magnetic Hybrid Nanostructures: Preparation, Properties, and Applications in Biology. *IEEE Trans. Nanobiosci.* **2007**, *6*, 298−308.

(9) Wang, G.; Su, X. The Synthesis and Bio-applications of Magnetic and Fluorescent Bifunctional Composite Nanoparticles. *Analyst* **2011**, *136*, 1783−1798.

(10) Yen, S. K.; Padmanabhan, P.; Selvan, S. T. Multifunctional Iron Oxide Nanoparticles for Diagnostics, Therapy and Macromolecule Delivery. *Theranostics* **2013**, *3*, 986−1003.

(11) Menon, J. U.; Jadeja, P.; Tambe, P.; Vu, K.; Yuan, B.; Nguyen, K. T. Nanomaterials for Photo-based Diagnostic and Therapeutic Applications. *Theranostics* **2013**, *3*, 152−166.

DOI: 10.1021/acsami.5b07515
ACS Appl. Mater. Interfaces 2015, 7, 23373−23386

(12) Shi, D.; Sadat, M. E.; Dunn, A. W.; Mast, D. B. Photo-fluorescent and Magnetic Properties of Iron Oxide Nanoparticles for Biomedical Applications. *Nanoscale* **2015**, *7*, 8209−8232.
(13) Lacroix, L. − M.; Delpech, F.; Nayral, C.; Lachaize, S.; Chaudret, B. New Generation of Magnetic and Luminescent Nanoparticles for *in Vivo* Real-time Imaging. *Interface Focus* **2013**, *3*, 20120103.
(14) Ali, Z.; Abbasi, A. Z.; Zhang, F.; Arosio, P.; Lascialfari, A.; Casula, M. F.; Wenk, A.; Kreyling, W.; Plapper, R.; Seidel, M.; Niessner, R.; Knöll, J.; Seubert, A.; Parak, W. J. Multifunctional Nanoparticles for Dual Imaging. *Anal. Chem.* **2011**, *83*, 2877−2882.
(15) Wang, D.; He, J.; Rosenzweig, N.; Rosenzweig, Z. Superparamagnetic Fe_2O_3 Beads−CdSe/ZnS Quantum Dots Core−shell Nanocomposite Particles for Cell Separation. *Nano Lett.* **2004**, *4*, 409−413.
(16) Bertorelle, F.; Wilhelm, C.; Roger, J.; Gazeau, F.; Ménager, C.; Cabuil, V. Fluorescence-modified Superparamagnetic Nanoparticles: Intracellular Uptake and Use in Cellular Imaging. *Langmuir* **2006**, *22*, 5385−5391.
(17) Sahoo, Y.; Goodarzi, A.; Swihart, M. T.; Ohulchanskyy, T. Y.; Kaur, N.; Furlani, E. P.; Prasad, P. N. Aqueous Ferrofluid of Magnetite Nanoparticles: Fluorescence Labeling and Magnetophoretic Control. *J. Phys. Chem. B* **2005**, *109*, 3879−3885.
(18) Holzapfel, V.; Lorenz, M.; Weiss, C. K.; Schrezenmeier, H.; Landfester, K.; Mailänder, V. Synthesis and Biomedical Applications of Functionalized Fluorescent and Magnetic Dual Reporter Nanoparticles as Obtained in the Miniemulsion Process. *J. Phys.: Condens. Matter* **2006**, *18*, S2581−S2594.
(19) Sathe, T. R.; Agrawal, A.; Nie, S. Mesoporous Silica Beads Embedded with Semiconductor Quantum Dots and Iron Oxide Nanocrystals: Dual-function Microcarriers for Optical Encoding and Magnetic Separation. *Anal. Chem.* **2006**, *78*, 5627−5632.
(20) Makovec, D.; Čampelj, S.; Bele, M.; Maver, U.; Zorko, M.; Drofenik, M.; Jamnik, J.; Gaberšček, M. Nanocomposites Containing Embedded Superparamagnetic Iron Oxide Nanoparticles and Rhodamine 6G. *Colloids Surf., A* **2009**, *334*, 74−79.
(21) Chekina, N.; Horák, D.; Jendelová, P.; Trchová, M.; Bene, M. J.; Hrubý, M.; Herynek, V.; Turnovcová, K.; Syková, E. Fluorescent Magnetic Nanoparticles for Biomedical Applications. *J. Mater. Chem.* **2011**, *21*, 7630−7639.
(22) Lattuada, M.; Hatton, T. A. Synthesis, Properties and Applications of Janus Nanoparticles. *Nano Today* **2011**, *6*, 286−308.
(23) Hu, J.; Zhou, S.; Sun, Y.; Fang, X.; Wu, L. Fabrication, Properties and Applications of Janus Particles. *Chem. Soc. Rev.* **2012**, *41*, 4356−4378.
(24) Macková, H.; Horák, D.; Trachtová, S.; Rittich, B.; Španová, A. The Use of Magnetic Poly(*N*-isopropylacrylamide) Microspheres for Separation of DNA from Probiotic Dairy Products. *J. Colloid Sci. Biotechnol.* **2012**, *1*, 235−240.
(25) Charoenmark, L.; Polpanich, D.; Thiramanas, R.; Tangboriboonrat, P. Preparation of Superparamagnetic Polystyrene-based Nanoparticles Functionalized by Acrylic Acid. *Macromol. Res.* **2012**, *20*, 590−596.
(26) Rahman, M. M.; Montagne, F.; Fessi, H.; Elaissari, A. Anisotropic Magnetic Microparticles from Ferrofluid Emulsion. *Soft Matter* **2011**, *7*, 1483−1490.
(27) Alam, M. A.; Rabbi, M. A.; Miah, M. A. J.; Rahman, M. M.; Rahman, M. A.; Ahmad, H. A Versatile Approach on the Preparation of Dye-labeled Stimuli-responsive Composite Polymer Particles by Surface Modification. *J. Colloid Sci. Biotechnol.* **2012**, *1*, 225−234.
(28) Poletto, F. S.; Fiel, L. A.; Lopes, M. V.; Schaab, G.; Gomes, A. M. O.; Guterres, S. S.; Rossi-Bergmann, B.; Pohlmann, A. R. Fluorescent-labeled Poly(ε-caprolactone) Lipid-core Nanocapsules: Synthesis, Physicochemical Properties and Macrophage Uptake. *J. Colloid Sci. Biotechnol.* **2012**, *1*, 89−98.
(29) Gaponik, N.; Radtchenko, I. L.; Sukhorukov, G. B.; Rogach, A. L. Luminescent Polymer Microcapsules Addressable by a Magnetic Field. *Langmuir* **2004**, *20*, 1449−1452.
(30) Yang, J.; Lim, E. − K.; Lee, H. J.; Park, J.; Lee, S. C.; Lee, K.; Yoon, H. − G.; Suh, J. − S.; Huh, Y. − M.; Haam, S. Fluorescent Magnetic Nanohybrids as Multimodal Imaging Agents for Human Epithelial Cancer Detection. *Biomaterials* **2008**, *29*, 2548−2555.
(31) Yuet, K. P.; Hwang, D. K.; Haghgooie, R.; Doyle, P. S. Multifunctional Superparamagnetic Janus Particles. *Langmuir* **2010**, *26*, 4281−4287.
(32) Yin, S. − N.; Wang, C. − F.; Yu, Z. − Y.; Wang, J.; Liu, S. − S.; Chen, S. Versatile Bifunctional Magnetic-fluorescent Responsive Janus Supraballs towards the Flexible Bead Display. *Adv. Mater.* **2011**, *23*, 2915−2919.
(33) Hu, S. − H.; Gao, X. Nanocomposites with Spatially Separated Functionalities for Combined Imaging and Magnetolytic Therapy. *J. Am. Chem. Soc.* **2010**, *132*, 7234−7237.
(34) Hong, X.; Li, J.; Wang, M.; Xu, J.; Guo, W.; Li, J.; Bai, Y.; Li, T. Fabrication of Magnetic Luminescent Nanocomposites by a Layer-by-layer Self-assembly Approach. *Chem. Mater.* **2004**, *16*, 4022−4027.
(35) Ye, F.; Barrefelt, Å.; Asem, H.; Abedi-Valugerdi, M.; El-Serafi, I.; Saghafian, M.; Abu-Salah, K.; Alrokayan, S.; Muhammed, M.; Hassan, M. Biodegradable Polymeric Vesicles Containing Magnetic Nanoparticles, Quantum Dots and Anticancer Drugs for Drug Delivery and Imaging. *Biomaterials* **2014**, *35*, 3885−3894.
(36) Kaewsaneha, C.; Bitar, A.; Tangboriboonrat, P.; Polpanich, D.; Elaissari, A. Fluorescent-magnetic Janus Particles Prepared *via* Seed Emulsion Polymerization. *J. Colloid Interface Sci.* **2014**, *424*, 98−103.
(37) Gallagher, J. J.; Tekoriute, R.; O'Reilly, J. − A.; Kerskens, C.; Gun'ko, Y. K.; Lyncha, M. Bimodal Magnetic-fluorescent Nanostructures for Biomedical Applications. *J. Mater. Chem.* **2009**, *19*, 4081−4084.
(38) Bhattacharya, D.; Das, M.; Mishra, D.; Banerjee, I.; Sahu, S. K.; Maiti, T. K.; Pramanik, P. Folate Receptor Targeted, Carboxymethyl Chitosan Functionalized Iron Oxide Nanoparticles: A Novel Ultradispersed Nanoconjugates for Bimodal Imaging. *Nanoscale* **2011**, *3*, 1653−1662.
(39) Wang, B.; Hai, J.; Liu, Z.; Wang, Q.; Yang, Z.; Sun, S. Selective Detection of Iron(III) by Rhodamine-modified Fe_3O_4 Nanoparticles. *Angew. Chem., Int. Ed.* **2010**, *49*, 4576−4579.
(40) Ge, Y.; Zhang, Y.; He, S.; Nie, F.; Teng, G.; Gu, N. Fluorescence Modified Chitosan-coated Magnetic Nanoparticles for High-efficient Cellular Imaging. *Nanoscale Res. Lett.* **2009**, *4*, 287−295.
(41) Lim, E. − K.; Yang, J.; Dinney, C. P. N.; Suh, J. − S.; Huh, Y. − M.; Haam, S. Self-assembled Fluorescent Magnetic Nanoprobes for Multimode-biomedical Imaging. *Biomaterials* **2010**, *31*, 9310−9319.
(42) Kaewsaneha, C.; Opaprakasit, P.; Polpanich, D.; Smanmoo, S.; Tangboriboonrat, P. Immobilization of Fluorescein Isothiocyanate on Magnetic Polymeric Nanoparticle using Chitosan as Spacer. *J. Colloid Interface Sci.* **2012**, *377*, 145−152.
(43) Zhu, H.; Shang, Y.; Wang, W.; Zhou, Y.; Li, P.; Yan, K.; Wu, S.; Yeung, K. W. K.; Xu, Z.; Xu, H.; Chu, P. K. Fluorescent Magnetic Fe_3O_4/Rare Earth Colloidal Nanoparticles for Dual-modality Imaging. *Small* **2013**, *9*, 2991−3000.
(44) Zhu, H.; Tao, J.; Wang, W.; Zhou, Y.; Li, P.; Li, Z.; Yan, K.; Wu, S.; Yeung, K. W. K.; Xu, Z.; Xu, H.; Chu, P. K. Magnetic, Fluorescent, and Thermo-responsive Fe_3O_4/Rare Earth Incorporated Poly(St-NIPAM) Core−shell Colloidal Nanoparticles in Multimodal Optical/Magnetic Resonance Imaging Probes. *Biomaterials* **2013**, *34*, 2296−2306.
(45) Torkpur-Biglarianzadeh, M.; Salami-Kalajahi, M. Multilayer Fluorescent Magnetic Nanoparticles with Dual Thermoresponsive and pH-sensitive Polymeric Nanolayers as Anti-cancer Drug Carriers. *RSC Adv.* **2015**, *5*, 29653−29662.
(46) Yan, K.; Li, H.; Li, P.; Zhu, H.; Shen, J.; Yi, C.; Wu, S.; Yeung, K. W. K.; Xu, Z.; Xu, H.; Chu, P. K. Self-assembled Magnetic Fluorescent Polymeric Micelles for Magnetic Resonance and Optical Imaging. *Biomaterials* **2014**, *35*, 344−355.
(47) Kim, B.; Schmieder, A. H.; Stacy, A. J.; Williams, T. A.; Pan, D. Sensitive Biological Detection with a Soluble and Stable Polymeric Paramagnetic Nanocluster. *J. Am. Chem. Soc.* **2012**, *134*, 10377−10380.

DOI: 10.1021/acsami.5b07515
ACS Appl. Mater. Interfaces 2015, 7, 23373−23386

(48) Ahsan, A.; Aziz, A.; Arshad, M. A.; Ali, O.; Nauman, M.; Ahmad, N. M.; Elaissari, A. Smart Magnetically Engineering Colloids and Biothin Films for Diagnostics Applications. *J. Colloid Sci. Biotechnol* **2013**, *2*, 19−26.
(49) Rajaram, S.; Bhujbal, P.; Slipper, I. J.; Favretto, M. E.; Douroumis, D. Prostate Cancer Targeting with 7E11-C5.3-CdS Bioconjugated Quantum Dots. *J. Colloid Sci. Biotechnol.* **2013**, *2*, 34−39.
(50) Wang, F.; Li, J.; Wang, C. Hydrophilic and Fluorescent Colloidal Nanorods of MWNTs as Effective Targeted Drug Carrier. *J. Colloid Sci. Biotechnol.* **2012**, *1*, 192−200.
(51) Wu, L. Y.; Ross, B. M.; Hong, S.; Lee, L. P. Bioinspired Nanocorals with Decoupled Cellular Targeting and Sensing Functionality. *Small* **2010**, *6*, 503−507.
(52) Lee, H.; Yu, M. K.; Park, S.; Moon, S.; Min, J. J.; Jeong, Y. Y.; Kang, H. − W.; Jon, S.; Thermally Cross-linked; Superparamagnetic Iron. Oxide Nanoparticles: Synthesis and Application as a Dual Imaging Probe for Cancer. *J. Am. Chem. Soc.* **2007**, *129*, 12739−12745.
(53) Hałupka-Bryl, M.; Asai, K.; Thangavel, S.; Bednarowicz, M.; Krzyminiewski, R.; Nagasaki, Y. Synthesis and *in Vitro* and *in Vivo* Evaluations of Poly(ethyleneglycol)-*block*-poly(4-vinylbenzylphosphonate) Magnetic Nanoparticles containing Doxorubicin as a Potential Targeted Drug Delivery System. *Colloids Surf., B* **2014**, *118*, 140−147.
(54) Kim, K.; Kim, J. H.; Park, H.; Kim, Y. − S.; Park, K.; Nam, H.; Lee, S.; Park, J. H.; Park, R.-W.; Kim, I. − S.; Choi, K.; Kim, S. Y.; Park, K.; Kwon, I. C. Tumor- homing Multifunctional Nanoparticles for Cancer Theragnosis: Simultaneous Diagnosis, Drug Delivery, and Therapeutic Monitoring. *J. Controlled Release* **2010**, *146*, 219−227.
(55) Lee, C. − M.; Jang, D.; Kim, J.; Cheong, S. − J.; Kim, E. − M.; Jeong, M. − H.; Kim, S. − H.; Kim, D. W.; Lim, S. T.; Sohn, M. − H.; Jeong, Y. Y. f.; Jeong, H. − J. Oleyl-chitosan Nanoparticles Based on a Dual Probe for Optical/MR Imaging. *Bioconjugate Chem.* **2011**, *22*, 186−192.
(56) Liu, C.; Gao, Z.; Zeng, J.; Hou, Y.; Fang, F.; Li, Y.; Qiao, R.; Shen, L.; Lei, H.; Yang, W.; Gao, M. Magnetic/upconversion Fluorescent $NaGdF_4$:Yb,Er Nanoparticle-based Dual-modal Molecular Probes for Imaging Tiny Tumors *in Vivo*. *ACS Nano* **2013**, *7*, 7227−7240.
(57) Wang, G.; Peng, Q.; Li, Y. Lanthanide-doped Nanocrystals: Synthesis, Optical-magnetic Properties, and Applications. *Acc. Chem. Res.* **2011**, *44*, 322−332.
(58) Nitin, N.; LaConte, L. E. W.; Zurkiya, O.; Hu, X.; Bao, G. Functionalization and Peptide-based Delivery of Magnetic Nanoparticles as an Intracellular MRI Contrast Agent. *JBIC, J. Biol. Inorg. Chem.* **2004**, *9*, 706−712.
(59) Yin, C.; Hong, B.; Gong, Z.; Zhao, H.; Hu, W.; Lu, X.; Li, J.; Li, X.; Yang, Z.; Fan, Q.; Yao, Y.; Huang, W. Fluorescent Oligo(*p*-phenyleneethynylene) Contained Amphiphiles-encapsulated Magnetic Nanoparticles for Targeted Magnetic Resonance and Two-photon Optical Imaging *in Vitro* and *in Vivo*. *Nanoscale* **2015**, *7*, 8907−8919.
(60) Luk, B. T.; Zhang, L. Current Advances in Polymer-based Nanotheranostics for Cancer Treatment and Diagnosis. *ACS Appl. Mater. Interfaces* **2014**, *6*, 21859−21873.
(61) Xu, C.; Wang, B.; Sun, S. Dumbbell-like Au−Fe_3O_4 Nanoparticles for Target-specific Platin Delivery. *J. Am. Chem. Soc.* **2009**, *131*, 4216−4217.
(62) Sotiriou, G. A.; Hirt, A. M.; Lozach, P. − Y.; Teleki, A.; Krumeich, F.; Pratsinis, S. E. Hybrid, Silica-coated, Janus-like Plasmonic-magnetic Nanoparticles. *Chem. Mater.* **2011**, *23*, 1985−1992.
(63) Fan, Z.; Senapati, D.; Singh, A. K.; Ray, P. C. Theranostic Magnetic Core−plasmonic Shell Star Shape Nanoparticle for the Isolation of Targeted Rare Tumor Cells from Whole Blood, Fluorescence Imaging, and Photothermal Destruction of Cancer. *Mol. Pharmaceutics* **2013**, *10*, 857−866.
(64) Abbasi, A. Z.; Prasad, P.; Cai, P.; He, C.; Foltz, W. D.; Amini, M. A.; Gordijo, C. R.; Rauth, A. M.; Wu, X. Y. Manganese Oxide and Docetaxel co-loaded Fluorescent Polymer Nanoparticles for Dual Modal Imaging and Chemotherapy of Breast Cancer. *J. Controlled Release* **2015**, *209*, 186−196.

DOI: 10.1021/acsami.5b07515
ACS Appl. Mater. Interfaces 2015, 7, 23373−23386